ELSEVIER

Agricultural and Forest Meteorology 115 (2003) 31–50

AGRICULTURAL AND FOREST METEOROLOGY

www.elsevier.com/locate/agrformet

Calculation of winds disturbed by an array of fences

John D. Wilson [a,*], Eugene Yee [b]

[a] *Department of Earth & Atmospheric Sciences, University of Alberta, Edmonton, Alberta, Canada T6G 2E3*
[b] *Defense Research Establishment (Suffield), Medicine Hat, Alberta, Canada*

Accepted 26 June 2002

Abstract

It is known that when an isolated porous windbreak is represented by a sink in the mean momentum equations, even the simplest turbulence closures lead to reasonably good simulations of the mean wind close to the barrier, irrespective of whether or not sources are introduced in the turbulent kinetic energy (TKE) and dissipation rate (ϵ) equations. However, unless the barrier is considered to dissipate TKE in addition to opposing the mean flow, the pattern of turbulence is poorly simulated.

Here we examine the performance of simple Reynolds-averaged Navier–Stokes (RANS) wind models for the case of a windbreak *network*, relative to the field experiment of McAneney and Judd (15 porous fences, height $h = 2$ m, spaced at $D_x/h = 6$ along the mean wind). *All* closures we considered gave mediocre predictions even for the mean flow, contrasting with the case of an isolated barrier; while, just as for the isolated barrier, prediction of the TKE in a windbreak network hinges on ambiguous choices in the treatment of TKE (and ϵ) sources at the barriers.

The additional turbulence generated by a sequence of barriers implies that a proper representation of the Reynolds stress is more critical than in the case of an isolated barrier, near which the pressure-gradient force dominates. This surely accentuates the importance of the turbulence closure, and our results *may* imply that no existing RANS turbulence closure is adequate for this type of flow. However, the problem could alternatively stem from the treatment of sinks parameterising the flow–fence interaction, not only in the TKE and ϵ-equations (where perforce such terms are heuristic), but even in the momentum equations.

Keywords: Windbreak; Shelter; Shelterbelt; Wind models; Shelter fence; Turbulence closures; RANS models

1. Introduction

In some regions of the world, for example, parts of New Zealand and France, arrays of windbreaks are vital in specialized agriculture and horticulture. For almost a century, and perhaps even longer, the scientific study of windbreaks has been motivated by the search for the most effective types of and usages of windbreaks, for a diverse range of benefits including reduced soil erosion, higher canopy temperatures, or reduced fruit motion. Early work is reviewed by van Eimern et al. (1964), and a more up-to-date survey is given by Brandle et al. (1988).

Wind and micro-climate models express in the most general way our understanding of disturbed flows, for in principle all particular cases lie within their compass. Standard turbulence models have proven able to simulate quite well the mean flow and (not so unambiguously) the turbulent kinetic energy (TKE) about a long, *isolated*, porous windbreak standing on flat ground (Wilson, 1985; Wang and Takle, 1995; Packwood, 2000; Wilson et al., 2001). But this article

* Corresponding author. Tel.: +1-403-492-3265; fax: +1-403-492-2030.
E-mail address: jaydee.uu@ualberta.ca (J.D. Wilson).

0168-1923/02/$ – see front matter
PII: S0168-1923(02)00169-7

will present evidence that may imply the aerodynamics of *multiple* porous barriers eludes existing (Reynolds-averaged Navier–Stokes (RANS)) models.

Early attempts to extract a general understanding of the principal aerodynamic effects of windbreaks were empirical, field and wind tunnel experiments contributing many valuable qualitative insights. In parallel with the experimental work, some scientists treated the windbreak as a problem in turbulent fluid mechanics, and appropriately so, for an isolated windbreak constitutes one of the canonical disturbances of an ideal atmospheric surface layer (others being the step change in surface roughness z_0, and the step change in surface energy-flux densities Q^*, Q_H, Q_E).

As early examples, both Tani (1958) and Kaiser (1959) correctly treated a windbreak as a source of mean velocity-deficit $\Delta\bar{u}$, but they treated $\Delta\bar{u}$ as a passive scalar. This means that the spatial distribution of $\Delta\bar{u}$ was controlled by turbulent diffusion along the vertical, and advection by the approach flow $\bar{u}_0(z)$, i.e. terms that are non-linear in the velocity disturbance were ignored. These treatments also missed the essential influence of the pressure field, which is responsible for the displacement of the location of minimum mean velocity downwind from the windbreak. Continuing experiments, steadily improving in their fidelity (e.g. Raine and Stevenson, 1977), emphasized the deficiencies of the early numerical treatments, although perhaps the theoretical studies helped make experimentalists more aware of the requirements for similitude, and the value of giving an *aerodynamic* characterization of the windbreak itself, rather than previous qualitative, visual descriptions ('very dense', 'permeable', or 'thin from top to bottom').

With growing accessibility of computing power, and the incursion of numerical fluid mechanics into micro-meteorology, e.g. Taylor's (1970) early treatment of local advection over surface temperature changes, came more plausible simulations of windbreak flows, using RANS models. Using the k–ϵ closure, Durst and Rasogi (1980) calculated the effects of a *solid* barrier, requiring that mean velocity vanish at the barrier. Also using the k–ϵ closure, Hagen et al. (1981) treated a *porous* fence, by imposing a measured mean velocity profile in the immediate wake of the fence.

Wilson (1985) reverted to the representation of a porous barrier as a momentum sink, involving the (easily measurable) resistance coefficient (k_r) of the material, and showed that good predictions of the mean wind field near an *isolated* windbreak could be obtained. This was the case irrespective of the complexity of the turbulence closure, presumably due to the dominating influence of the pressure gradient near the fence. However, further downwind, where the pressure gradient has relaxed and is less important than the turbulent shear stress, these simulations, regardless of closure, slightly underestimated the rate of recovery of the wind: thus Wilson (1985) concluded that 'one could not with confidence simulate the more complex problem of a windbreak network'.

Nevertheless similar calculations by Wang and Takle (1995) did not manifest this problem. Wilson and Mooney (1997) sought to discover why not, and thought the better performance of Wang and Takle's model *may* have been ascribable to a too-shallow computational domain. However, it is probably a fruitless distraction to focus unduly on small differences between simulations, especially when observations themselves are scarce and carry their own uncertainty.

The question posed here is this: may we say that today's RANS models satisfactorily describe the wind in an *array* of windbreaks? In what follows a tentative answer will be given, from a comparison of simulations of the wind in an array of fences with the corresponding observations of McAneney and Judd (1991).

2. Experiments on arrays of windbreaks

In view of the practical importance of windbreak arrays, the paucity of experimental data relating specifically to their aerodynamic performance is surprising. van Eimern et al. (1964) noted that 'systematic experiments for this problem demand numerous parallel belts of the same kind on an even, uniform ground, which has so far only been possible in the wind tunnel and at small belts'. They questioned 'whether the results gained with a single belt are applicable, and which is the best interval for the belts' and observed that 'a simple application of the results gained before cannot be enough, because a system of several belts alters the roughness of the land ... An extensive system of wind protection leads to a new equilibrium of the flow owing to the greater roughness of the surface'.

Seguin and Gignoux (1974) nicely brought out this latter point in a comparison of the mean wind profile (at $z \leq 12$ m) observed downwind of a succession of hedges (height $h = 8$ m) spaced at intervals $D_x/h =$ 4–5, against the corresponding profile amid a large open area (airport). They showed that in the lee of the hedges the neutral wind profile displayed a 'kink', demarcating an inner region (or internal boundary layer (IBL)) from an outer region. The inner region was characterized by a small roughness length and a local friction velocity u'_* that was *reduced* relative to the reference value u_* at the airport. However, the mean velocities above the inner region implied an apparent roughness length that was large (of order $h/10$), and a friction velocity u''_* *exceeding* the reference value. Iqbal et al. (1977) systematically studied the roughness and displacement lengths of the equilibrium wind profile developed by a series of equi-spaced, non-porous barriers in a naturally-developed wall shear layer within a wind tunnel. Varying the windbreak spacing D_x/h from 1 to 20, they determined that maximum roughness occurs with $D_x/h = 3$.

Judd et al. (1996) carried out a wind tunnel simulation of the flow through porous windbreaks standing in a model plant canopy[1] ($h/h_c \approx 3$, where h_c is crop height), the barriers being spaced at intervals of $D_x/h = 6$ or 12. In the case $D_x/h = 6$, the array consisted of a total of seven windbreaks, three upwind and three downwind from the central break, about which measurements were focused. According to Judd et al., the upstream members of an array of windbreaks may be considered as 'an additional upstream roughness' having two main consequences: 'an overall decrease in windspeed ... due to upwind (windbreaks)'; and 'an increase in ambient turbulence leading to a decrease in the shelter efficiency of any one break in a multiple array relative to an equivalent single break'. These findings are consistent with earlier studies of windbreak arrays, the increased levels of turbulence having been noted by Woodruff and Zingg (1955), who in the context of their wide-ranging interest in wind erosion, reported mean windspeed and turbulence intensity within a flow domain defined by four consecutive porous fences (field and wind tunnel observations).

From their study, Judd et al. concluded that the 'non-local' shelter afforded by an array as a whole dominates the reduced effectiveness of any *one* of its members due to enhanced turbulence (which causes faster recovery of the velocity in the wake of any *one* member of the array), observing 'windspeeds within a multiple array that are smaller than those behind a single windbreak, given identical external conditions'. However, the increased turbulence is a serious limitation to the use of shelterbelts for some purposes, and particularly in the context of plant or fruit movement.

McAneney and Judd (1991) measured mean wind (using cup anemometers) and turbulence (using a one-dimensional sonic anemometer) in their unique field study of the windflow about a series of 15 very long, parallel fences (their 'aeolian array'). The site was flat and unobstructed (roughness length $z_0 =$ 0.007 m, displacement height $d = 0.045$ m), and data were selected for near-neutral stratification, with the mean wind direction within 10° of normal to the fences. The fences were composed of a porous, plastic windbreak cloth, had height $h = 2$ m ($h/z_0 = 290$), and were spaced along-wind at intervals $D_x/h = 6$. McAneney and Judd concluded with the observation that 'in a practical sense, the data clearly demonstrate the difficulty of simultaneously reducing both mean windspeeds and turbulence at crop levels using repeated windbreaks at conventional horticultural spacings'.

The above survey covers virtually all existing observations useful in judging models and theories of micro-meteorological flow in an array of porous barriers. Of these, the data of McAneney and Judd have been chosen as a criterion for the simulations to follow. This is because the wind tunnel study of Judd et al. (1996) is more complex, due to having included a plant canopy, and more especially because of other uncertainties that would have arisen in attempting a simulation, e.g. due to the fact that some members of the windbreak array actually stood, not in the canopy, but in the inflow (metal tombstones) or outflow (gravel) regions of the flow.

[1] Patton et al. (1998) reported an LES study of this experiment, approximating the repeated windbreaks by assuming flow through a *single* fence in a domain terminated by periodic along-wind boundary conditions. Patton et al. concluded that 'mean fields from the numerical and physical simulations show striking resemblances', but that velocity variances were not simulated quite so well. Thus, LES, though computationally far more demanding than RANS, does provisionally appear promising for the calculation of disturbed flows.

3. Governing equations for numerical simulations of winds in an array of fences

Because this paper hopes to draw a general inference on the capability of micro-meteorological models for highly disturbed flows, it is necessary that the models investigated should include representative closures that span the range available, i.e. several variants of eddy viscosity closures, as well as stress closures.

As will become clear, primarily we parameterize the interaction of the wind with a fence (or fences) by means of a sink in the momentum equations. But while there is some evidence that this step is satisfactory, the corresponding sources and sinks that (could) appear in the various supporting equations (such as equations for the TKE and TKE dissipation rate ϵ, if required by the closure) are much less certain. It is known, however, that these choices are crucial: without a TKE sink, for example, simulations do not produce the region of reduced turbulence in the lee of a porous fence (Wilson, 1985; Packwood, 2000).

3.1. Symmetries, assumptions and the key variables

We let x denote a coordinate aligned with the mean wind, and let the windbreak(s) be infinitely long and aligned cross-wind, i.e. along the cross-wind (y) direction. Assume the surface layer approaching the windbreak(s) is neutrally-stratified, and that the wind flow is stationary, i.e. *statistics* of the wind are invariant in time. The statistical properties which stand for 'knowledge' of the wind include the mean velocity components $\bar{u} = \bar{u}(x, z)$, $\bar{w} = \bar{w}(x, z)$, and statistics of the turbulent fluctuations relative to these means, i.e. the vertical flux of momentum $\overline{u'w'}$ and the turbulent velocity variances ($\overline{u'^2}$, etc.), whose sum gives the turbulent kinetic energy $k = (1/2)(\overline{u'^2} + \overline{v'^2} + \overline{w'^2})$. Governing equations for the state variables are derived by Reynolds-averaging the Navier–Stokes equations.

3.2. Mean momentum equations and momentum sinks

The governing equation for $\bar{u}$ is:

$$\frac{\partial}{\partial x}\left(\bar{u}^2 + \overline{u'^2} + \bar{p}\right) + \frac{\partial}{\partial z}(\bar{u}\bar{w} + \overline{u'w'}) = S_{\bar{u}}, \qquad (1)$$

where $\bar{p}$ is the disturbance in mean kinematic pressure, generated by the interaction of the wind with obstacles. The LHS is simply the divergence of the mean flux ($\overrightarrow{F_u}$) of u-momentum, and so Eq. (1) could be written symbolically as:

$$\frac{\partial \bar{u}}{\partial t} = 0 = -\nabla \cdot \overrightarrow{F_u} + S_{\bar{u}}. \qquad (2)$$

In reference to a small cube of airspace, the term $\nabla \cdot \overrightarrow{F_u}$ measures the *net* rate of transport of $\bar{u}$-momentum across the walls, while $S_{\bar{u}}$ represents production or destruction of momentum inside the cube. In the present case the momentum sink $S_{\bar{u}}$ represents the drag of the N fences, and may be parameterized as:

$$S_{\bar{u}} = -k_r \bar{u}\sqrt{\bar{u}^2 + \bar{w}^2}\, s(z - h) \sum_{k=1}^{N} \delta(x - x_{fk}), \qquad (3)$$

where k_r is the (dimensionless) resistance coefficient of the fence(s), $s(z - h)$ is a dimensionless step function (1 for $z \leq h$ and 0 for $z > h$) and the delta-functions specify the x-wise locations (x_{fk}) of fences, numbered $k = 1, \ldots, N$. A corresponding sink is included in the $\bar{w}$-momentum equation, but its effect has been found to be negligible, whether in the case of a single fence or an array.

From Eq. (1) it is obvious that the velocity fluctuations impact the mean velocity $\bar{u}_j$ through the Reynolds stress $\overline{u'_i u'_j}$, but turbulence also impacts the mean velocity through its influence on the mean pressure. In *models*, the feedback of the computed turbulence field on the computed mean velocity depends in detail on the closure assumptions.

RANS wind simulations couple Eq. (1) with the vertical momentum equation, the incompressible continuity equation, and a "turbulence closure" whose role is to provide the impact of the unresolved (turbulent) eddies on the mean flow. Before outlining the closures tested here, we first consider the impact of porous barriers on velocity fluctuations.

3.3. TKE sources arising from interaction of the wind with a fence

If a porous barrier is treated as a momentum sink, in lieu of imposing correct boundary conditions on the true (complex, three-dimensional) geometry and fully resolving the flow at the fence, an important consequence is that there are additional turbulent

kinetic energy sources and sinks. Firstly, the drag forces convert kinetic energy of the mean flow (MKE) to turbulent kinetic energy in some range of scales of motion ('wake scales', WKE); and secondly the fluctuating drag extracts energy from the eddies, re-depositing it in the wake scales (a spectral-transfer mechanism which acts in parallel with the normal vortex-stretching mechanism).

In vegetation canopies wake scales of motion are usually considered to be 'small', and thus rapidly dissipated. Although it is sometimes possible to detect a hump or peak in the power spectrum, reflecting the deposition of energy into wake scales, measurements reviewed by Seginer et al. (1976) led them to regard "eddies generated by branches and leaves as only a small perturbation on the main spectrum" and to conclude that "only a small fraction of the turbulence which can be observed inside natural canopies has its origin in the wakes of individual elements".

Thus, for convenience in modeling such flows, Wilson (1988) split the turbulence spectrum into two bands (k, k_w) where k is the 'shear kinetic energy' (SKE) and k_w the 'wake kinetic energy' (WKE). MKE lost to the drag forces was assumed to be re-deposited as WKE, while the SKE $\rightarrow$ WKE term was modeled heuristically as:

$$\epsilon = \epsilon_{cc} + \epsilon_{fd} = \frac{(c_e k)^{3/2}}{\lambda} + \frac{1}{2} C_d A \bar{u} (4\overline{u'^2} + 2\overline{v'^2} + 2\overline{w'^2}), \quad (4)$$

where A is the leaf area density (m^{-1}) and λ the turbulence length scale. The first term represents the conventional vortex-stretching mechanism (ϵ_{cc} for 'cascade conversion'). The second term (ϵ_{fd}) is due to the action of the form drag on vegetation, and was derived by assuming that momentum sinks of form $C_d A(u^2, uv, uw)$ appear in the *instantaneous* momentum equations.[2] In the present context where the drag is exerted by a porous fence rather than a continuum of vegetation, we may substitute $k_r s(z-h)\delta(x-x_f)$ for the $C_d A$ product, postponing consideration of whether "wake scales" of motion actually are unimportant, and whether spectral division is appropriate. Then the corresponding SKE sinks in the individual variance-budget equations would be (omitting the localising functions):

$$\epsilon_{xx} = 4k_r \bar{u} \overline{u'^2} + \tfrac{2}{3}\epsilon_{cc},$$
$$\epsilon_{yy} = 2k_r \bar{u} \overline{v'^2} + \tfrac{2}{3}\epsilon_{cc}, \quad (5)$$
$$\epsilon_{zz} = 2k_r \bar{u} \overline{w'^2} + \tfrac{2}{3}\epsilon_{cc}.$$

Wilson's treatment of the stress tensor departed from the Launder et al. (1975; LRR) closure it derived from, in several respects. Normal components of the stress tensor were considered as representing the SKE band (only); canopy sinks were included, and a closure coefficient was arbitrarily modified. The usual ϵ_{cc}-equation was not carried, ϵ_{cc} being parameterized directly using the equilibrium form shown above; of course the closure then relied on an imposed length scale.

Ayotte et al. (1998; AFR) gave a turbulence closure for plant canopies differing in several respects[3] from that of Wilson (1988), and we have performed some calculations in line with their scheme. As with Wilson's closure the dissipation rate is split into two terms, but to prescribe ϵ_{cc} AFR retain (and merely modify) the usual ϵ-equation.

To estimate the instantaneous drag forces, AFR replaced Wilson's projections (uu, uv, uw) with the rigorous form $(u|\vec{u}|, v|\vec{u}|, w|\vec{u}|)$, where $|\vec{u}| \equiv (u_i u_i)^{1/2}$ is the magnitude of the instantaneous velocity vector $\vec{u}$. Then the instantaneous drag terms are:

$$S_{u_i} = -k_r u_i [u_j u_j]^{1/2} s(z-h) \sum_{k=1}^{N} \delta(x - x_{fk}). \quad (6)$$

To facilitate ensemble-averaging, one may 'linearize' the non-linear portion of the instantaneous drag term

[2] Consideration that, at the fences, space is 'multiply-connected' will show that indeed, an extra source term must be included (Wilson and Shaw, 1977; Wilson et al., 1990). It can be shown that a term of this form in the instantaneous momentum equations implies loss of energy at *all* scales, which is not quite realistic, since there must be a compensating production of TKE at "wake" scales.

[3] Refined treatment of drag forces; inclusion of LRR ϵ-equation; closure reduces to standard LRR second-order closure, in absence of vegetation.

as follows:

$$
\begin{aligned}
&[(\bar{u}_j + u'_j)(\bar{u}_j + u'_j)]^{1/2}(\bar{u}_i + u'_i) \\
&\quad = M\left(1 + 2\frac{\bar{u}_j u'_j}{M^2} + \frac{u'_j u'_j}{M^2}\right)^{1/2}(\bar{u}_i + u'_i) \\
&\quad \approx M\left(1 + \frac{\bar{u}_j u'_j}{M^2}\right)(\bar{u}_i + u'_i) \\
&\quad \approx M(\bar{u}_i + u'_i) + \frac{\bar{u}_i \bar{u}_j}{M} u'_j, \qquad (7)
\end{aligned}
$$

where $M \equiv (\bar{u}_i \bar{u}_i)^{1/2} = \sqrt{\bar{u}^2 + \bar{w}^2}$ is the magnitude of the mean velocity vector, and we have neglected all terms involving products of turbulent velocity fluctuations of order two or greater. Then we recover a source term:

$$
S_{\bar{u}_i} = -k_r \bar{u}_i M s(z-h) \sum_{k=1}^{N} \delta(x - x_{fk}) \qquad (8)
$$

in the ith mean momentum equation [cf. Eq. (3)]. Correspondingly, we retrieve a source/sink term in the transport equation for TKE that has the following form, assuming that the Reynolds stresses are modeled using the Boussinesq K-closure (to follow):

$$
\begin{aligned}
\epsilon_{fd} &= k_r \left[\frac{8}{3} Mk - 2K \frac{\bar{u}_i \bar{u}_j}{M} \frac{\partial \bar{u}_i}{\partial x_j}\right] s(z-h) \\
&\quad \times \sum_{k=1}^{N} \delta(x - x_{fk}). \qquad (9)
\end{aligned}
$$

This source/sink contribution to the TKE transport equation is obtained by the usual manipulation.[4] The first term in the square brackets of Eq. (9) is always positive, and hence leads to an additional mechanism for the reduction of TKE at the barriers. However, the second term, which depends on the mean velocities and their gradients, has an indefinite sign and can act either as a source or sink in the TKE transport equation.

"Spectral division" is a heuristic approach to parameterizing turbulence in RANS models when a form drag term (distributed mean-momentum sink) appears in the momentum equations. In the present case of windflow about porous barriers, it is not clear that it is appropriate to consider that MKE (and large-scale TKE) lost to the form drag should reappear as (unimportant) small-scale TKE, i.e. there may well be *large* scales of WKE. Thus, the conceptual advantage of Wilson's two-band TKE treatment is dubious and one might prefer to consider that k represents the *entire spectrum of turbulent motion*. In that case an MKE → TKE source term (in its simplest guise, $k_r \bar{u}^3$) must appear in its budget equation. Furthermore since fluctuating drag forces merely change the scale of the turbulent eddies, it would be wrong in principle to include the form drag sink ϵ_{fd}. As far as we know, no calculation of this type has ever captured the "quiet zone" in the lee of a windbreak; on the contrary, such calculations normally have the outcome that TKE in the lee of a barrier is *increased*, due to the conversion of the MKE.

Finally, lest including a TKE sink in windbreak simulations still seems opportunistic, please note that the application of rapid-distortion theory to the passage of a uniform, weakly turbulent ($\sigma_u/\bar{u} \ll 1$), confined stream through a fine mesh, as in a wind tunnel, agrees well with observations that all three components of the turbulence are damped (Batchelor, 1953). Of course, the tenets of rapid-distortion theory do not apply to the natural windbreak (high turbulence intensity, mean shear).

3.4. First-order closures

The Boussinesq eddy viscosity (K) closure:

$$
\overline{u'_i u'_j} = -K\left(\frac{\partial \bar{u}_i}{\partial x_j} + \frac{\partial \bar{u}_j}{\partial x_i}\right) + \frac{2}{3} k \delta_{ij}, \qquad (10)
$$

is often a useful approximation for the shearing stresses, e.g.:

$$
\overline{u'w'} = -K(x,z)\left(\frac{\partial \bar{u}}{\partial z} + \frac{\partial \bar{w}}{\partial x}\right), \qquad (11)
$$

but is less satisfactory with respect to normal stresses, and so adjustments (that violate the ij-symmetry) are often introduced. We shall show simulations of wind about multiple windbreaks using the following variants of the K closure.

[4] First find the transport equation for the velocity fluctuation u'_i by subtracting the mean momentum equation from the instantaneous momentum equation; multiply the resulting equation by u'_j; set $i = j$ and sum over i; ensemble-average.

3.4.1. Eddy viscosity of the approach flow ("K_0")

Wilson (1985) showed that, for a single barrier, quite good simulations of the mean wind (less good for the turbulence) result by setting:

$$K(x,z) = K_0(z) = k_v u_{*0} z, \tag{12}$$

where u_{*0} is the friction velocity of the approach flow and k_v is von Kármán's constant ("K_0-closure"). Where we tested this treatment of the eddy viscosity, we simplified the momentum equations, viz.:

$$\frac{\partial}{\partial x}\left(\bar{u}^2 - K_a \frac{\partial \bar{u}}{\partial x}\right) + \frac{\partial}{\partial z}\left(\bar{w}\bar{u} - K_0(z)\frac{\partial \bar{u}}{\partial z}\right) = -\frac{\partial \bar{p}}{\partial x} + S_{\bar{u}}, \tag{13}$$

where K_a is a small "artificial diffusivity". The rationale for an artificial diffusivity is to emphasize that the Boussinesq closure for the *normal* stresses is unrealistic; since K_a is small, in effect the normal stress gradients are neglected in this treatment.

3.4.2. One-equation closure: imposed length scale ("K_k")

As what they regarded as the "simplest turbulence closure that will adequately describe changes to the mean wind field, particularly very close to ground, in flow over hilly, forested terrain", Wilson et al. (1998; WFR) explored the classical first-order closure:

$$K(x,z) = \lambda (c_e k)^{1/2}, \tag{14}$$

where k is the turbulent kinetic energy, calculated from its simplified governing differential equation, and $\lambda = \lambda(x,z)$ is an algebraic length scale. With the simplest formula for λ capable of reproducing the flow structure in and above the canopy, this closure performed as well or better than earlier, more complex closures for flow over a ridge, and was later applied by Wilson and Flesch (1999) to interpret measured wind variations in a periodic series of forest clearings (see also Pinard and Wilson, 2001).

WFR chose the $K \propto \lambda k^{1/2}$ closure "to avoid complicated turbulence schemes, however popular, whose basis is especially weak in the case of a canopy flow (e.g. the ϵ-equation)". For the same reasons, we here test this closure for the flow through a sequence of porous barriers, setting:

$$\lambda = k_v z. \tag{15}$$

(Any number of heuristic adjustments of λ could have been tried.)

For calculations testing this formulation of the eddy viscosity, we used Eq. (13), and the analogous form for a $\bar{w}$-equation; the associated TKE equation was:

$$\frac{\partial}{\partial x}\left(\bar{u}k - K_a \frac{\partial k}{\partial x}\right) + \frac{\partial}{\partial z}\left(\bar{w}k - \frac{K}{\sigma_k}\frac{\partial k}{\partial z}\right) = K\left(\frac{\partial \bar{u}}{\partial z} + \frac{\partial \bar{w}}{\partial x}\right)^2 - \epsilon, \tag{16}$$

where K_a is the "artificial diffusivity" and σ_k is the ratio of the eddy viscosity to the transport coefficient for TKE. The computed TKE field feeds back on the computed mean velocity field only through its impact on the "true" eddy viscosity applied to calculate the shear stress.

We have split the TKE dissipation rate[5] as:

$$\epsilon = \epsilon_{cc} + \epsilon_{fd}, \tag{17}$$

and parameterized ϵ_{cc} conventionally as:

$$\epsilon_{cc} = \frac{(c_e k)^{3/2}}{\lambda}. \tag{18}$$

In conjunction with this K_k closure, rather than use Eq. (9) we specified the TKE sink due to form drag by the simpler prescription:

$$\epsilon_{fd} = \alpha\, k_r\, \bar{u}\, k\, s(z-h) \sum_{k=1}^{N} \delta(x - x_{fk}), \tag{19}$$

where α is a constant of order 1 (Wilson, 1985). Note that where using this closure we consider that k excludes wake-scale TKE, and so we do not include MKE → TKE conversion.

3.4.3. Two-equation closures: standard k–ϵ model and variants

By far the most popular two-equation closure is the k–ϵ model in which model transport equations are solved for the TKE (k) and the viscous dissipation rate (ϵ) from which can be formed a turbulence length scale $\lambda = k^{3/2}/\epsilon$ and an eddy viscosity:

$$K(x,z) = C_\mu \frac{k^2}{\epsilon}, \tag{20}$$

[5] Whereas WFR set $\epsilon = \max[\epsilon_{cc}, \epsilon_{fd}]$. The distinction is inconsequential.

where C_μ is one of five model constants. In this paper, the k–ϵ model will be used within a linear eddy viscosity framework, i.e. used with the Boussinesq linear constitutive relationship between stress and strain[6] as expressed in Eq. (10), and without simplification of the mean momentum equations, in contrast with the previously-described K_0 and K_k closures. Please note too that in our calculations ϵ_{cc} always substitutes for ϵ in the definition of the eddy viscosity, except where otherwise stated.

The TKE is determined from:

$$\frac{\partial}{\partial x}\left(\bar{u}k - \frac{K}{\sigma_k}\frac{\partial k}{\partial x}\right) + \frac{\partial}{\partial z}\left(\bar{w}k - \frac{K}{\sigma_k}\frac{\partial k}{\partial z}\right) = P_k - \epsilon, \tag{21}$$

and ϵ from:

$$\frac{\partial}{\partial x}\left(\bar{u}\epsilon - \frac{K}{\sigma_\epsilon}\frac{\partial \epsilon}{\partial x}\right) + \frac{\partial}{\partial z}\left(\bar{w}\epsilon - \frac{K}{\sigma_\epsilon}\frac{\partial \epsilon}{\partial z}\right) = \frac{\epsilon}{k}(C_{\epsilon 1}P_k - C_{\epsilon 2}\epsilon). \tag{22}$$

In these equations, P_k is the shear production term modeled within the Boussinesq eddy viscosity approximation as:

$$P_k = K\left[2\left(\left(\frac{\partial \bar{u}}{\partial x}\right)^2 + \left(\frac{\partial \bar{w}}{\partial z}\right)^2\right) + \left(\frac{\partial \bar{u}}{\partial z} + \frac{\partial \bar{w}}{\partial x}\right)^2\right]. \tag{23}$$

It is simple to demonstrate that in a constant stress layer (e.g., log-law region of a wall-bounded turbulent flow) where (by assumption!) production and dissipation balance, Eq. (22) has the solution:

$$\epsilon = \frac{C_\mu^{3/4}k^{3/2}}{k_v z}, \tag{24}$$

with the closure constants related by:

$$k_v^2 = \sigma_\epsilon C_\mu^{1/2}(C_{\epsilon 2} - C_{\epsilon 1}). \tag{25}$$

[6] While the linear eddy viscosity hypothesis is reasonable in simple turbulent shear flows (e.g. boundary layer flow) where the turbulence characteristics and mean velocity gradients change slowly following the mean flow, it is known to be unrealistic in several classes of flows (e.g. strongly swirling flows, flows with significant streamline curvature, secondary motions that occur in straight ducts with non-circular cross-section). This has led to the development of a number of non-linear eddy viscosity models (e.g. Yoshizawa, 1984; Speziale, 1987; Rubinstein and Barton, 1990; Craft et al., 1996).

Comparing this result with Eq. (18), it is seen that $c_e = C_\mu^{1/2}$.

Different variants of the k–ϵ model arise depending on the different approaches used to determine the closure coefficients C_μ, σ_k, σ_ϵ, $C_{\epsilon 1}$, and $C_{\epsilon 2}$. Here, two forms will be investigated.

The standard k–ϵ model "$(k$–$\epsilon)_0$" employs values for the closure constants that have been arrived at by comprehensive data fitting for a wide range of 'canonical' turbulent flows, with the "standard" values of the constants given by:

$$C_\mu = 0.09, \quad \sigma_k = 1.0, \quad \sigma_\epsilon = 1.3, \quad C_{\epsilon 1} = 1.44, \quad C_{\epsilon 2} = 1.92. \tag{26}$$

These values of the constants correspond to a compromise chosen to give the "best" performance for a range of flows, and it is not likely that minor and/or ad hoc adjustments to their values would significantly affect the predictive accuracy.

We shall also present a simulation of windbreak flow using a more recent version of the k–ϵ model developed by Yakhot et al. (1992) using the renormalization group (RNG) procedure. In the RNG model "$(k$–$\epsilon)_{RNG}$":

$$C_\mu = 0.085, \quad \sigma_k = 0.72, \quad \sigma_\epsilon = 0.72, \tag{27}$$

$$C_{\epsilon 1} = 1.42 - \frac{\eta(1 - \eta/\eta_0)}{1 + \beta\eta^3}, \quad C_{\epsilon 2} = 1.68, \tag{28}$$

where

$$\beta = 0.012, \quad \eta_0 = 4.377, \quad \eta \equiv (P_k/K)^{1/2}\frac{k}{\epsilon}. \tag{29}$$

This functional dependence of $C_{\epsilon 1}$ on the non-dimensional characteristic strain rate η is an empirical result, the value of the adjustable constant β having been set using near-wall turbulence data. It is this ad hoc adjustment of $C_{\epsilon 1}$ that is largely responsible for differences in performance between the standard and RNG models.

We shall report simulations using the $(k$–$\epsilon)_0$ and $(k$–$\epsilon)_{RNG}$ closures entirely without additional source or sink terms in the k and ϵ-equations, as discussed in the previous section (such simulations are designated "Model 1"). We also investigate two different methodologies for incorporating form drag source/sink terms

in the model transport equations for k and ϵ (cf. Eqs. (21) and (22)).

Results designated "Model 2" treat k as if spectrally divided; such simulations resemble model "K_k", but accept literally the Boussinesq closure for the normal stresses, and model ϵ_{cc} using the transport equation. The inclusion of the earlier-derived source/sink term in the transport equation for TKE yields:

$$\begin{aligned}&\frac{\partial}{\partial x}\left(\bar{u}k-\frac{K}{\sigma_k}\frac{\partial k}{\partial x}\right)+\frac{\partial}{\partial z}\left(\bar{w}k-\frac{K}{\sigma_k}\frac{\partial k}{\partial z}\right)\\&\quad=P_k-\epsilon_{cc}-k_r\left[\frac{8}{3}Mk-\frac{2K}{M}\left(\bar{u}^2\frac{\partial\bar{u}}{\partial x}\right.\right.\\&\qquad\left.\left.+\bar{u}\,\bar{w}\left(\frac{\partial\bar{u}}{\partial z}+\frac{\partial\bar{w}}{\partial x}\right)+\bar{w}^2\frac{\partial\bar{w}}{\partial z}\right)\right]\\&\qquad\times\left(s(z-h)\sum_{k=1}^{N}\delta(x-x_{fk})\right).\end{aligned}\tag{30}$$

The modeled transport equation for ϵ_{cc} cannot be derived systematically from the unaveraged Navier–Stokes equation. Essentially, it is a dimensionally consistent analogy to the associated TKE transport equation (Eq. (30)):

$$\begin{aligned}&\frac{\partial}{\partial x}\left(\bar{u}\epsilon_{cc}-\frac{K}{\sigma_\epsilon}\frac{\partial\epsilon_{cc}}{\partial x}\right)+\frac{\partial}{\partial z}\left(\bar{w}\epsilon_{cc}-\frac{K}{\sigma_\epsilon}\frac{\partial\epsilon_{cc}}{\partial z}\right)\\&\quad=\frac{\epsilon_{cc}}{k}(C_{\epsilon1}P_k-C_{\epsilon2}\epsilon_{cc})\\&\quad+\frac{\epsilon_{cc}}{k}\left\{C_{\epsilon1}\frac{2K}{M}\left[\bar{u}^2\frac{\partial\bar{u}}{\partial x}+\bar{u}\bar{w}\left(\frac{\partial\bar{u}}{\partial z}+\frac{\partial\bar{w}}{\partial x}\right)+\bar{w}^2\frac{\partial\bar{w}}{\partial z}\right]\right.\\&\qquad\left.-C_{\epsilon2}\frac{8}{3}Mk\right\}\left(k_r s(z-h)\sum_{k=1}^{N}\delta(x-x_{fk})\right).\end{aligned}\tag{31}$$

Note that in Eq. (31), the portion of the source/sink term in the TKE equation that has indefinite sign has been incorporated with the term multiplied by $C_{\epsilon1}$ ('production of dissipation'), whereas the portion of the source/sink term in the TKE equation that has a positive definite sign has been incorporated with the term multiplied by $C_{\epsilon2}$ ('dissipation of dissipation').

Finally, k–ϵ simulations identified as "Model 3" are the k–ϵ analog of the second-order closure model proposed by Ayotte et al. (1998) for plant canopy flows. Here, the total dissipation is split according to Eq. (17) and ϵ_{fd} is determined according to Eq. (9). In addition to the inclusion of ϵ_{fd} as a sink term in the TKE transport equation, Model 3 includes the MKE → TKE transfer term as (AFR):

$$P_{MKE}=\frac{1}{2}k_r M^3 s(z-H)\sum_{k=1}^{N}\delta(x-x_{fk}).\tag{32}$$

Hence, for Model 3, the TKE transport equation assumes the following form:

$$\begin{aligned}&\frac{\partial}{\partial x}\left(\bar{u}k-\frac{K}{\sigma_k}\frac{\partial k}{\partial x}\right)+\frac{\partial}{\partial z}\left(\bar{w}k-\frac{K}{\sigma_k}\frac{\partial k}{\partial z}\right)\\&\quad=P_k-\epsilon_{cc}+P_{MKE}\\&\quad-k_r\left[\frac{8}{3}Mk-\frac{2K}{M}\left(\bar{u}^2\frac{\partial\bar{u}}{\partial x}+\bar{u}\,\bar{w}\left(\frac{\partial\bar{u}}{\partial z}+\frac{\partial\bar{w}}{\partial x}\right)\right.\right.\\&\qquad\left.\left.+\bar{w}^2\frac{\partial\bar{w}}{\partial z}\right)\right]\left(s(z-h)\sum_{k=1}^{N}\delta(x-x_{fk})\right),\end{aligned}\tag{33}$$

where the eddy viscosity is defined here using the *total* dissipation ϵ, i.e. $K\equiv C_\mu k^2/(\epsilon_{cc}+\epsilon_{fd})$. Ayotte et al. advocate the use of the *total* dissipation (i.e. ϵ) for the determination of the eddy viscosity in this equation (and, also in the transport equation for ϵ_{cc}), arguing that this is required to model the "reduction of the lifetime of energy containing eddies compared to the 'no-canopy' case" that arises due to the interaction of the flow with the canopy.

The free-air dissipation ϵ_{cc} in Model 3 is modeled using the conventional transport equation for TKE dissipation rate (cf. Eq. (22)), with ϵ_{cc} replacing ϵ everywhere in the equation except in the determination of the eddy viscosity K. Hence:

$$\begin{aligned}&\frac{\partial}{\partial x}\left(\bar{u}\epsilon_{cc}-\frac{K}{\sigma_\epsilon}\frac{\partial\epsilon_{cc}}{\partial x}\right)+\frac{\partial}{\partial z}\left(\bar{w}\epsilon_{cc}-\frac{K}{\sigma_\epsilon}\frac{\partial\epsilon_{cc}}{\partial z}\right)\\&\quad=\frac{\epsilon_{cc}}{k}(C_{\epsilon1}P_k-C_{\epsilon2}\epsilon_{cc}),\end{aligned}\tag{34}$$

with (again) $K\equiv C_\mu k^2/(\epsilon_{cc}+\epsilon_{fd})$.

Here we have but rippled the surface of the ocean of variants of the k–ϵ closure!

3.5. Rao–Wyngaard–Coté second-order closure

The Rao–Wyngaard–Coté (RWC) local advection model (Rao et al., 1974a,b; Bink, 1996; Wilson et al.,

2001) uses a second-order closure that is not very different from other common second-order closures. In particular, it differs from LRR principally in that it does not parameterize the "rapid" part of the pressure strain. Under neutral stratification, RWC consists of coupled equations for $\bar{u}$, $\bar{w}$, $\overline{u'^2}$, $\overline{v'^2}$, $\overline{w'^2}$, $\overline{u'w'}$, and the mean pressure $\bar{p}$ and TKE dissipation rate ϵ.

The prognostic equation for $\overline{u'^2}$ ($\equiv \sigma_u^2$) is:

$$\frac{\partial}{\partial x}\left(\bar{u}\sigma_u^2 - a_t\tau\sigma_u^2\frac{\partial\sigma_u^2}{\partial x}\right) + \frac{\partial}{\partial z}\left(\bar{w}\sigma_u^2 - a_t\tau\sigma_w^2\frac{\partial\sigma_u^2}{\partial z}\right) = -2\sigma_u^2\frac{\partial\bar{u}}{\partial x} - 2\overline{u'w'}\frac{\partial\bar{u}}{\partial z} - \frac{c_{11}}{\tau}\left(\sigma_u^2 - \frac{2}{3}k\right) + \frac{\partial}{\partial x}\left(a_t\tau\overline{u'w'}\frac{\partial\sigma_u^2}{\partial z}\right) + \frac{\partial}{\partial z}\left(a_t\tau\overline{u'w'}\frac{\partial\sigma_u^2}{\partial x}\right) - \frac{2}{3}\epsilon_{cc} - \epsilon_{fdx}. \quad (35)$$

In Eq. (35), a_t and c_{11} are closure coefficients, $\tau = 2k/\epsilon_{cc}$ is a turbulence timescale, and for the present calculations the $\overline{u'^2}$ sink term ϵ_{fdx} is given by (cf Eq. (5)):

$$\epsilon_{fdx} = 4k_r\bar{u}\sigma_u^2 s(z-h)\sum_{k=1}^{N}\delta(x - x_{fk}). \quad (36)$$

The flow disturbance is "driven" by the sink terms $S_{\bar{u}}$ and ϵ_{fdx} in the $\bar{u}$- and σ_u^2-equations.

Away from the fences, dissipation of TKE is entirely due to the normal vortex-cascade mechanism, and the RWC ϵ-equation is:

$$\bar{u}\frac{\partial\epsilon_{cc}}{\partial x} + \bar{w}\frac{\partial\epsilon_{cc}}{\partial z} = -2a\frac{\epsilon_{cc}}{k}\overline{u_i'u_k'}\frac{\partial\bar{u}_i}{\partial x_k} - 2\frac{\epsilon_{cc}^2}{k} + 2a_t^{\epsilon}\frac{\partial}{\partial x_k}\left(\frac{k}{\epsilon_{cc}}\overline{u_k'u_l'}\frac{\partial\epsilon_{cc}}{\partial x_l}\right), \quad (37)$$

where $a = 1/2$ (and the summation convention applies). This is similar to the ϵ-equations of other well-known closures, and provided the coefficients are appropriately chosen, for the equilibrium state it will result in:

$$\epsilon_{cc} = \frac{(c_e k)^{3/2}}{k_v z} = \frac{u_*^3}{k_v z}. \quad (38)$$

Note that in application here of the RWC closure, no additional sinks or sources of ϵ_{cc} have been inserted due to the presence of the fences. For reasons of numerical accuracy, we transformed Eq. (37) into an equation for the product $(z\epsilon_{cc})$.

From this section, it must be clear that there is ambiguity as to what are the proper sources in TKE and ϵ-equations. It is for this reason that we have covered a range of choices, including closures that are too näive even to contain those equations.

4. Previous simulations of a single fence

Before presenting simulations of a windbreak *array*, it is pertinent to remind the reader of the promising performance of RANS models for a *single* barrier.

4.1. Bradley and Mulhearn's fence

Bradley and Mulhearn (1983; BM83) carried out an experiment on neutral flow through a very long, isolated, porous fence standing on uniform ground, parameters being $h = 1.2$ m, $z_0 = 0.002$ m ($h/z_0 = 600$), and $k_r = 2$. Fig. 1 is a simulation of this experiment. The domain was $-10 \le x \le 100$ m, $z \le 50$ m, and gridlengths were $\Delta x = 1$ m, $\Delta z = 0.15$ m ($\Delta x/h = 0.83$, $\Delta z/h = 0.125$, i.e. very close to the resolution used for the simulations of a windbreak array which follow). Fig. 1 is similar to the result reported by Wilson et al. (2001, Fig. 2), and the differences are consequences of a minor change in the program: the $\bar{u}$-momentum sink specified by Eq. (3) involves the projection of the square of the mean velocity on the x-axis, whereas in the earlier program the sink was simply $-k_r\bar{u}^2$.

Wilson (1985) had given similar results for the BM83 fence, using a range of closures. Other RANS simulations of the BM83 fence followed, including those by Wang and Takle (1995), Wilson and Mooney (1997), and Lee (2001).

4.2. Ellerslie fence

Wilson (1987) compared observations of the along-wind profile of mean ground-level pressure $\bar{p}_0(x)$ upwind and downwind from a single porous plastic fence on bare ground ($h = 1.25$ m, $z_0 = 0.008$ m, $h/z_0 = 160$, $k_r = 2.4$), with a simulation using the LRR second-order closure. Modeled mean pressure was in reasonable agreement with the observations.

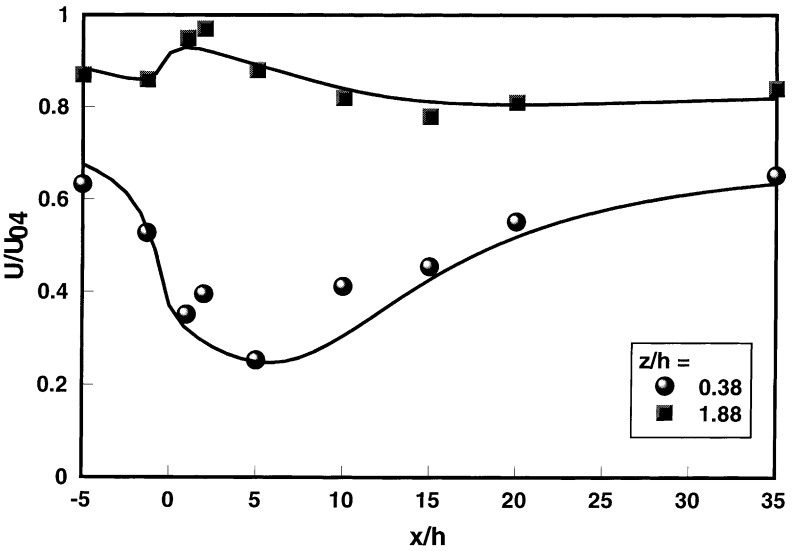

Fig. 1. Solution of the RWC local advection model for mean wind reduction by an infinitely-long porous fence standing at $x = 0$, in neutrally-stratified flow at perpendicular incidence. Symbols give field observations of Bradley and Mulhearn (1983), for the case ($h/z_0 = 600$, $k_r = 2$), and U_{04} is the mean windspeed observed upstream from the fence at $z = 4$ m.

4.3. Surrey wind tunnel fence

Packwood (2000) compared simulations using a proprietary CFD code against others' wind tunnel experiments, with two-dimensional solid and porous (23 and 50%) fences. Packwood considered that, regarding previous experiments on flow through a porous fence, "none give sufficiently detailed data of either the upstream or downstream flows to permit comparison with CFD modeling without some estimate of one or more of the inlet (upstream) quantities". On first sight this appears a surprising statement because, for example, in the experiment of BM83, all necessary details of the (neutral) atmospheric surface layer flow are known, and the normalized mean velocity statistics were reported in detail. However, the comment is justified by Packwood's careful focus on "determining a suitable resistance model for a given geometry where often only a crude estimate of the volumetric porosity is available". That is, Packwood considers the aerodynamic parameterization of the BM83 fence to be incomplete, or ambiguous, for he correctly distinguishes between the drag of a porous screen "not in the presence of walls or immersed in a boundary layer", versus the drag in situ of a real fence. This is potentially an important point, for Wilson (1985) had proceeded by *assuming* an adequate estimate of the resistance coefficient of a fence (in its atmospheric condition) could be had by blocking a uniform, non-turbulent stream with a (full-scale) section of the actual fence. We shall return to this point later.

Here focusing on the results for porous fences, in Packwood's simulations the fence itself was represented as having a finite thickness, spanning about 3 "cells" of a total of about 200 cells along the streamwise axis (this means the region of favorable pressure gradient and flow acceleration within the material is explicitly represented, whereas in the Wilson (1985) approach the fence is represented by a delta-function source). The drag coefficient of the porous region was inferred from earlier measurements. Computations were reported using both a k–ϵ closure and, alternatively, a Reynolds stress closure; the standard k–ϵ closure is well known to over-predict production of TKE near stagnation points, thus in flows about bluff bodies, and so in Packwood's computations, a modified ϵ-equation was used.

Regarding prediction of the mean velocity field, Packwood found that both the closures he examined performed almost equally well (results were shown for

$x/h = 1, 8$). This is consistent with Wilson (1985) (who also considered a range of closures) and the hypothesis[7] that the flow disturbance near the fence is dominated by the influence of the strong adverse pressure-gradient. Predicted profiles of the Reynolds stress $\overline{u'w'}$ at $x/h = 1$ were about equally skillful, but at $x/h = 8$ the Reynolds stress closure gave clearly superior results; again, this is completely consistent with Wilson (1985).

Finally, Packwood noted that while in reality there is a region of reduced turbulence ("quiet zone") in the lee of an isolated porous fence, his simulations with the Reynolds stress closure over-predicted $\overline{u'^2}$ in that region. Wilson (1985) had noted that the LRR closure does not capture the reduced turbulence in the quiet zone unless a TKE sink at the fence is included. Packwood does not state whether in his simulations the fences were taken to imply additional sources or sinks of TKE and ϵ, but from his results it seems not.

Thus we conclude that there is a remarkable harmony of results across these two independent examinations of the competence of numerical fluid mechanics for the case of an isolated porous barrier, with (of particular relevance for this paper) consistent consequences for the inclusion (or otherwise) of fence drag modifications of the TKE and ϵ-equations.

5. Simulations of the McAneney–Judd windbreak array

A sample of the windbreak cloth, provided by Dr. McAneney, was placed in a wind tunnel (Department of Mechanical Engineering, University of Alberta) in order to determine its resistance coefficient:

$$k_r = \frac{\Delta p}{\rho U^2}, \tag{39}$$

i.e. the pressure drop Δp across the cloth, normalized by the scale ρU^2, where ρ is the air density, and U is the windspeed in the tunnel. Results were $k_r = 1.66$ (at $U = 11\,\mathrm{m\,s^{-1}}$) and $k_r = 1.74$ (at $U = 3.0\,\mathrm{m\,s^{-1}}$).

[7] This can be regarded as firmly established: solutions of momentum equations that entirely neglect perturbation Reynolds stresses capture well the mean wind effects to about $x/h \approx 5$ and even beyond.

5.1. Details of numerical method

For the simulations to be reported, the first of the 15 fences of the "aeolian array" was placed at $x/h = 0$, the 15th at $x/h = 84$, and the domain spanned $-25 \leq x/h \leq 150$. Along-wind resolution was $\Delta x = 1.5\,\mathrm{m}$ ($\Delta x/h = 0.75$), thus a $\bar{u}$ grid-point fell on each fence, with seven grid-points between each pair of fences. Vertical grid spacing was $\Delta z = 0.333\,\mathrm{m}$ ($\Delta z/h = 0.167$), and the domain depth $z_{mx}/h = 75$.

All the simulations except those involving the k–ϵ model used a staggered arrangement for velocity components and pressure on the grid (as in Wilson, 1985). The simulations with the k–ϵ model used a co-located, cell-centered procedure, i.e. all the dynamical variables were stored at the same set of grid points. The co-located arrangement of velocity components and pressure provokes chequerboard oscillations in the pressure field due to the velocity-pressure decoupling. To avoid this, the method of Rhie and Chow (1983) was used to interpolate cell face velocities from the nodal velocity values at the cell center. This non-linear interpolation essentially introduces a fourth-order "pressure diffusion" which smooths out the pressure oscillations.

Numerical method was a variation of SIMPLE (Patankar, 1980), as summarized by Wilson (1985). Within this scheme, the transport equations and the pressure-correction equations were solved sequentially and iterated to convergence. For all simulations except those involving the k–ϵ model, iterations continued until the whole-domain $\bar{u}$-momentum budget was satisfied to within 1% of the total windbreak drag in the domain. For the simulations using the k–ϵ model, a solution was assumed to have converged when the sums (over the whole-domain) of the absolute cell residuals, normalized by the respective total fluxes at the inflow (undisturbed upstream) plane, fell below 0.1%.

For all closures we checked that the specified inflow profiles

$$\begin{aligned} \frac{\bar{u}_0(z)}{u_{*0}} &= \log\left(\frac{z}{z_0}\right), \\ k_0(z) &= \frac{u_{*0}^2}{c_e}, \\ \epsilon_{cc_0}(z) &= \frac{u_{*0}^3}{k_v z}, \end{aligned} \tag{40}$$

were retained as the equilibrium solution, $\bar{u}(x,z) \approx \bar{u}_0(z)$, etc. after many iterations with $k_r = 0$ (no barriers).

5.2. Results of simulations

Fig. 2a–c compare the windspeed $\bar{u}(x,z)/\bar{u}_{0h}$ calculated by the models with that observed, at heights $z/h = 1/2, 2$. The high-resolution data at $37 \leq x/h \leq 41$ stem from the values of $\bar{u}(x,z)/\bar{u}_0(z)$ given by McAneney and Judd (1991, Table 1), from their observations between fences 7 (at $x/h = 36$) and 8; we re-scaled the given data for presentation in Fig. 2 by multiplying by $\ln[(z-d)/z_0]/\ln[(h-d)/z_0]$, with $d = 0.045$ m. The mean windspeeds deduced for $(x/h, z/h) = (39, 1/2)$ from McAneney and Judd's Fig. 1 and Table 1 are inconsistent (see footnote 8).

Fig. 2a shows that there is a wide spread in computed mean wind across the range of the simplest K-closures (K_0, K_k, $(k$–$\epsilon)_0$), with little sign of skill (relative to the observations) in any case. For the $K \propto \lambda k^{1/2}$ closure, results are shown with $\sigma_k = 5, \alpha = 1$ (the values used by WFR); however, results for the mean flow are not very different with the more usual choice $\sigma_k = 1$, nor do variations in α have much effect; in fact, calculated mean speeds with the $K \propto \lambda k^{1/2}$ closure showed almost no sensitivity to whether the TKE sink $S_{\mathrm{TKE}} \equiv -\epsilon_{\mathrm{fd}}$ was or was not included. It is also evident from Fig. 2a that the observed *modulation* (along-wind variation) in mean windspeed far exceeds that calculated by the numerical models.[8] Therefore, Fig. 1 of McAneney and Judd (1991) is slightly misleading, in that the interpolative line drawn between measured mean velocities at midpoints between widely-separated fences of the array does not reflect the (actually?) strongly modulated pattern in mean velocity between any two fences.

Fig. 2b shows that mean windspeeds calculated with the standard $(k$–$\epsilon)_0$ model are not very sensitive to differing treatments of sources and sinks in the k–ϵ-equations, while calculations with the $(k$-$\epsilon)_{RNG}$ model are distinct, but not better. Fig. 2c compares the standard $(k$–$\epsilon)_0$ closure (with sources treated by spectral division) with the RWC second-order closure.

From these results we can conclude that at $z/h = 1/2$, the calculations suggest *periodicity* downstream of about the fourth fence (but with a streamwise modulation that is much too small relative to that observed, as noted above), and do not show the slow but definitely continuing recovery in mean windspeed that was observed along the array; the $(k$–$\epsilon)_{\mathrm{RNG}}$ (Model 2) calculation is marginally superior in the latter respect. At $z/h = 2$, none of the calculations capture the observed minimum windspeed between the third and fourth fences, and slow recovery further to leeward. Perhaps the most definite conclusion from Fig. 2 is that differences between the various predictions are large, but all are in disaccord with the observations: does this imply that, of turbulence closures available to us, *none* is adequate for this flow?

The periodicity of the modeled mean wind field beyond about the fifth fence suggests that, to simulate the wind in the interior of the array (say, between fences 4 and 10) it would be acceptable to simulate a reduced number of fences, using higher resolution. Such a simulation, using the RWC closure, is shown (as a dotted line) in Fig. 2c; and except downwind of the (five) fences, is essentially identical to the simulation of the full array (the difference is largely if not all due to the fact that the gridpoint z_j falling closest to $z/h = 1/2$ differs between simulations). This result proves two points: that the full-array simulations can be regarded as essentially grid-independent; and, that the influence of the leeward ten fences on the flow about the windward five is negligible (a point which is fairly intuitive, and which has been observed many times in earlier studies).

In addition to their observations of the pattern in the mean wind about the aeolian array, McAneney and Judd reported the along-wind profile of the standard deviation σ_w in vertical velocity. Fig. 3 compares simulated and observed values of $\sigma_w(x,z)/\sigma_{w0}$. Unless a TKE sink is included, model predictions underestimate the spatial modulation in σ_w between the fences. If the TKE sink *is* included, then the models predict that the spatial modulation in σ_w is much stronger at lower heights, in agreement with the observations; and estimate the magnitude of that modulation quite well

[8] If the three leeward-most high-resolution observations in Fig. 2 were rescaled to ensure self-consistency between McAneney and Judd's Fig. 1 and Table 1, observed modulation would be more consistent with the models. A pre-publication report on the experiment by McAneney, Judd and Astill states "windspeed varies only by 13% between fences 7 and 8". This is far less than the modulation one infers from McAneney and Judd (1991), and which has been plotted here in Fig. 2a–c.

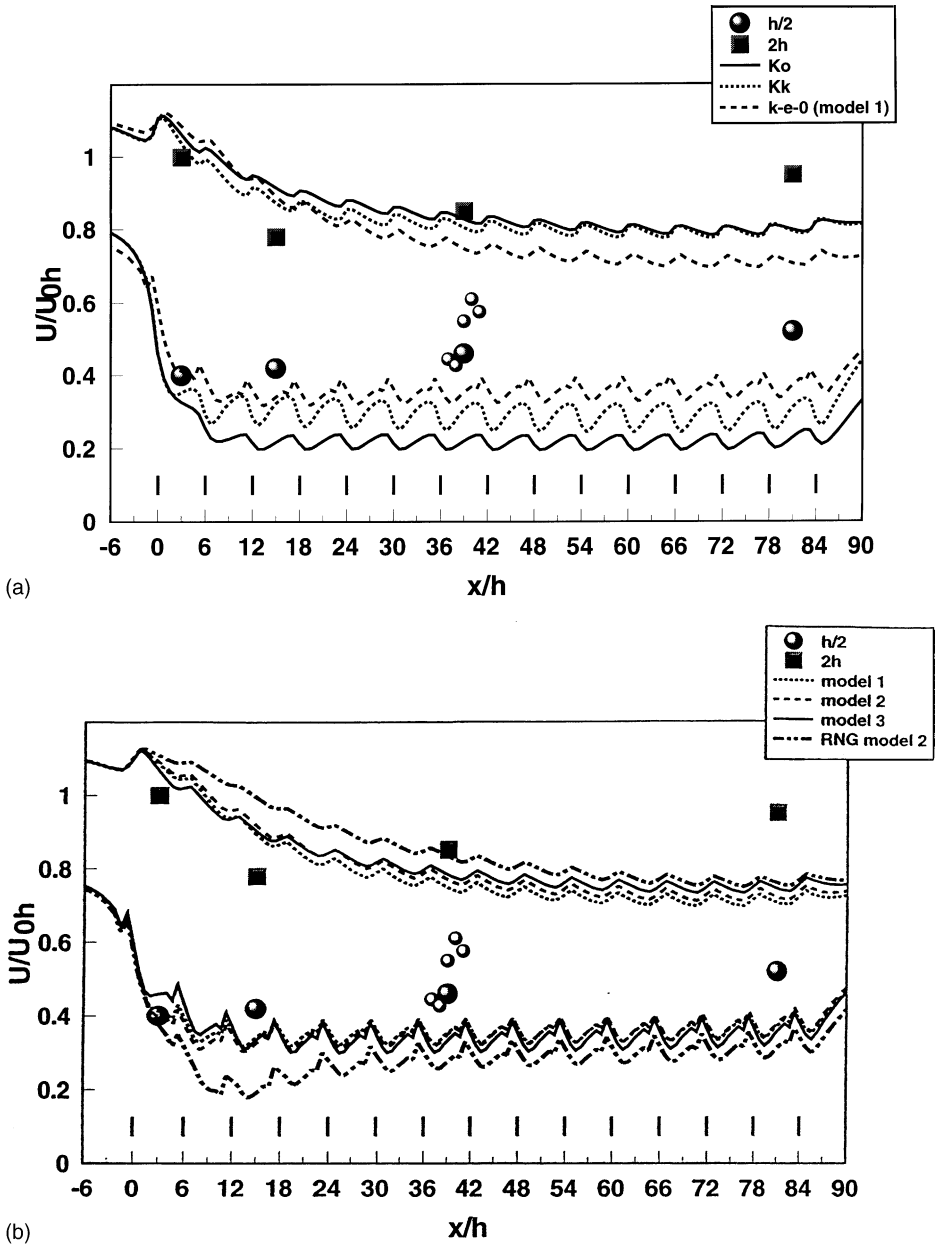

Fig. 2. (a) Simulated (lines) and observed (symbols) normalized mean windspeed U/U_{0h} within the 'aeolian array' of 15 windbreaks (McAneney and Judd, 1991). Parameters of the experiment were $h = 2\,\mathrm{m}$, $z_0 = 0.007\,\mathrm{m}$, $k_\mathrm{r} = 1.7$, and U_{0h} is the mean windspeed observed upstream from the fence at $z = h$. Computational resolution was $\Delta x = 1.5\,\mathrm{m}$, $\Delta z = 0.333\,\mathrm{m}$. Showing simulations with the simplest first-order closures. (b) As for (a). Simulations with k–ϵ closures and several treatments of TKE sources; standard k–ϵ model, except where labeled "RNG". (c) As for (a and b). Comparing simulations using the standard k–ϵ closure (Model 2) and the RWC closure. Computational resolution was $\Delta x = 1.5\,\mathrm{m}$, $\Delta z = 0.333\,\mathrm{m}$ except for the fine-dotted line, which is a finer-resolution simulation ($\Delta x = 0.75\,\mathrm{m}$, $\Delta z = 0.2\,\mathrm{m}$) with the RWC closure for the case where only the first five windbreaks are included.

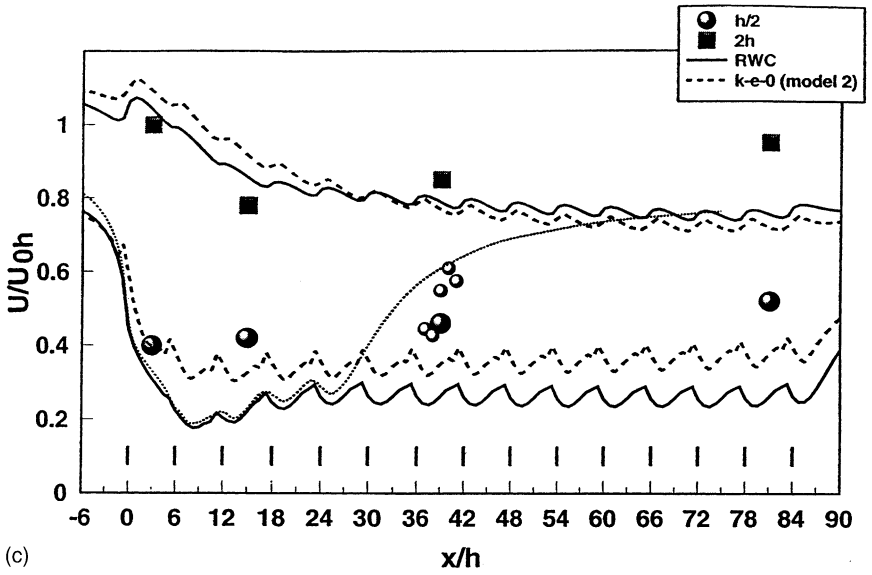

Fig. 2. (*Continued*).

at $z/h = (0.5, 1)$. The only other plus of the simulations with TKE sink is that they correctly indicate strong suppression of vertical exchange occurs *only* behind the first one or two fences, and near ground.

5.3. Discussion

Taken overall, the RANS simulations given above are ambiguous, and quite wrong relative to (these) observations. On the other hand there have been many demonstrations that, for sufficiently simple disturbances of the surface layer, RANS models are skillful. In the majority of such studies, admittedly, the flow to be simulated is 'known' experimentally, and so the simulations ultimately published *could* be the end result of an exercise that amounts to little more than 'fitting' curves (the mth variation of the nth model) to observations on a graph (we do subscribe to this viewpoint; on the contrary we consider RANS is objectively skillful, for simple flow disturbances). Furthermore, where models have been thoroughly 'tested' against observations, there is a tendency for the disturbances to be of the simplest character, e.g. disturbances where geometrical regularities prevail.

Cowan et al. (1997) and Sini et al. (1996) noted the concern that a given standard CFD 'package', e.g. the $(k–\epsilon)_0$ model, put in the hands of different users, throws up differing solutions of the same flow problem. This complicates the task of defining the inherent capability of RANS, but let us take the optimistic viewpoint that the present results, good or bad, reflect the inherent quality of the turbulence closure—not the numerical procedure, grid and domain choice, etc.[9] Then why should it be that RANS performs quite well for a single fence and quite poorly for an array of fences? This is perhaps the more surprising given that Wilson and Flesch (1999) showed that the $K \propto \sqrt{k}\lambda$ closure gave a credible simulation of flow through an array of forest blocks and clearings.[10]

[9] Regarding uncertainty in CFD, Roache (1997) distinguishes 'verification' as the assurance that one is 'solving the equations right' from 'validation' which has to do with assuring that one is 'solving the right equations'. In this paper, we suggest from our comparison of simulations against observations that the model(s) probably are *not* valid, i.e. *not* based on the right equations—which is perhaps not very surprising, in view of the well-known difficulty of properly parameterizing the Reynolds stresses.

[10] But here one must emphasize that, not knowing the effective drag coefficient $C_d Ah$ for their forest canopy strips, Wilson and Flesch treated this as a *free parameter*. Such a freedom, due to incomplete experimental data, is very common in comparison of micro-meteorological models and observations, and wherever exploited, must be seen as having compromised any claim to have *objectively* tested (or *validated*, Roache, 1997) a numerical model or theory.

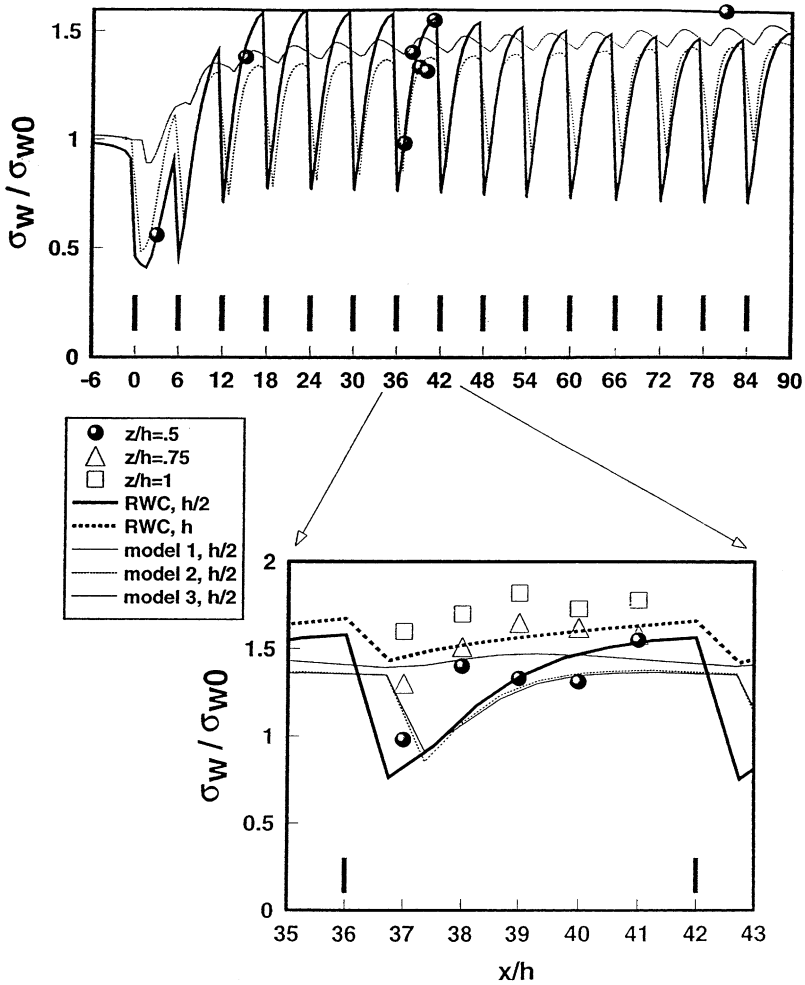

Fig. 3. Measured (symbols) and modeled (lines) along-wind profiles of the standard deviation of vertical velocity, $\sigma_w(x,z)/\sigma_{w0}$, in an array of 15 windbreaks, with blow-up emphasizing the variation between fences 7 and 8.

5.4. Possible reasons for poor agreement of multi-fence simulation with data

Firstly, how much confidence should be placed in the observations? The cup anemometers would surely have overestimated the mean speed, particularly in any region of high turbulence intensity. Fig. 4 shows a calculated horizontal profile of the turbulence intensity $\sigma_u(x,z)/\bar{u}(x,z)$ in the windbreak array, according to the RWC closure. At $z/h = 0.5$, the turbulence intensity exceeds 1/2 virtually everywhere, but still it is unlikely the cups should have overestimated by a factor of something like 50–200% (Wyngaard, 1981). Furthermore it is improbable that overspeeding could explain the *pattern* of the discrepancy between the observations and models at $z/h = 2$. However, there is reason to be suspicious of the reported between-fence modulation in mean speed, for the reason given earlier.

Secondly, could there be a problem with the primary parameterisation of the barriers, i.e. with the form of the imposed sinks in the momentum equations? Wilson et al. (1990) showed that inclusion of a localized momentum sink, neglecting the finite thickness of the mesh and the details of the flow within it,

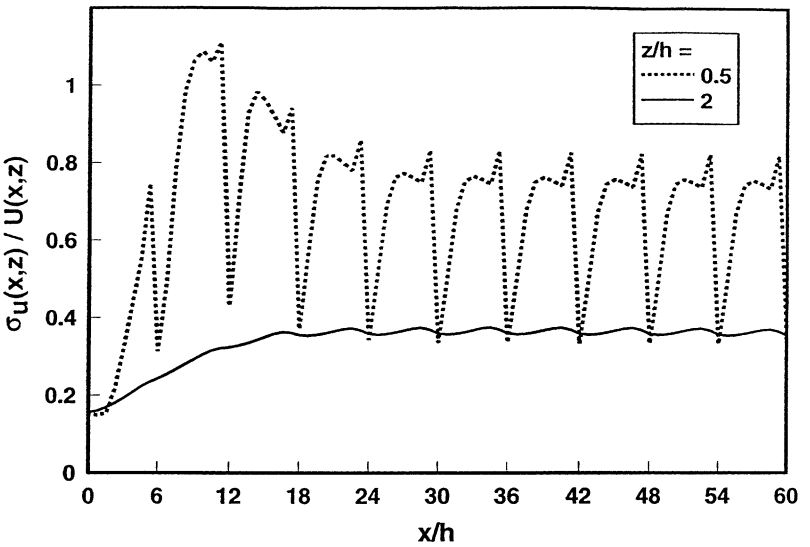

Fig. 4. Calculated along-wind profile of the turbulence intensity in the aeolian array, at $z/h = (1/2, 2)$, according to the RWC closure.

is a valid alternative to imposition of proper boundary conditions on the complex surface of a porous barrier. The sink, $k_r \bar{u}\sqrt{\bar{u}^2 + \bar{w}^2}$, is considered to estimate the mean (kinematic) back-pressure exerted locally by the barrier on the flow, in terms of the (height-variable) resolved mean wind "at" the barrier.

However, the resistance coefficient $k_r = k_r(\theta)$ is defined in reference to the passage of a laminar, uniform, confined stream through the (given) barrier, which is mounted at an angle θ with respect to the streamlines, and blocks the stream. Is it valid to carry over the numerical value of k_r from this non-turbulent "reference flow" and apply it to obtain the *mean* back pressure in a turbulent, unconfined stream?

The time-variability of the wind vector, and the non-normality and non-constancy of its orientation relative to the barrier, are the factors compromising the representation. At the *first* of a series of porous barriers, the mean angle of incidence of the wind $\bar{\theta} \approx \arctan(\bar{w}/\bar{u})$ at heights of order h is small ($<10^\circ$), but instantaneous values can be much bigger. Justification for the näive imposition of a resistance coefficient on the mean flow comes a posteriori—values of k_r deduced from shear-less laminar wind tunnel tests, when thus imposed in the mean momentum equations, lead to good agreement with field observations (Wilson, 1985). Surely this must imply that, even in the fluctuating real-world flow, the instantaneous pressure of the wind on an isolated fence can not be *too* different from $k_r \rho u\sqrt{u^2 + v^2 + w^2}$?

But what of the *further* complication (relative to the laminar reference flow) of barrier wakes impinging on downstream members of the array? Angles of attack on the second and later barriers probably exceed those at the first barrier, and turbulence intensities must be higher. Use of the same (constant) value of k_r for all members of an array (of physically-identical windbreaks) can be justified only by Occam's razor. One means to investigate this uncertainty in the treatment we have used here, would be large eddy simulation (LES), assigning each windbreak a resistance coefficient $k_r(u, v, w)$ applied to the instantaneous (resolved) wind (u, v, w), and varying realistically with angle of attack.

There is no need to repeat the discussion of our uncertainty relative to sources and sinks in the TKE and ϵ-equations, other than to record again that consequences for the calculated *mean* flow do not seem sufficiently important to explain the collective discrepancy of the simulations relative to the observations.

Finally, if none of the above mechanisms explain the poor simulation, it seems necessary to conclude (tentatively) that the turbulence closures surveyed are *all* unrealistic. Is this at all plausible? Fig. 5 shows

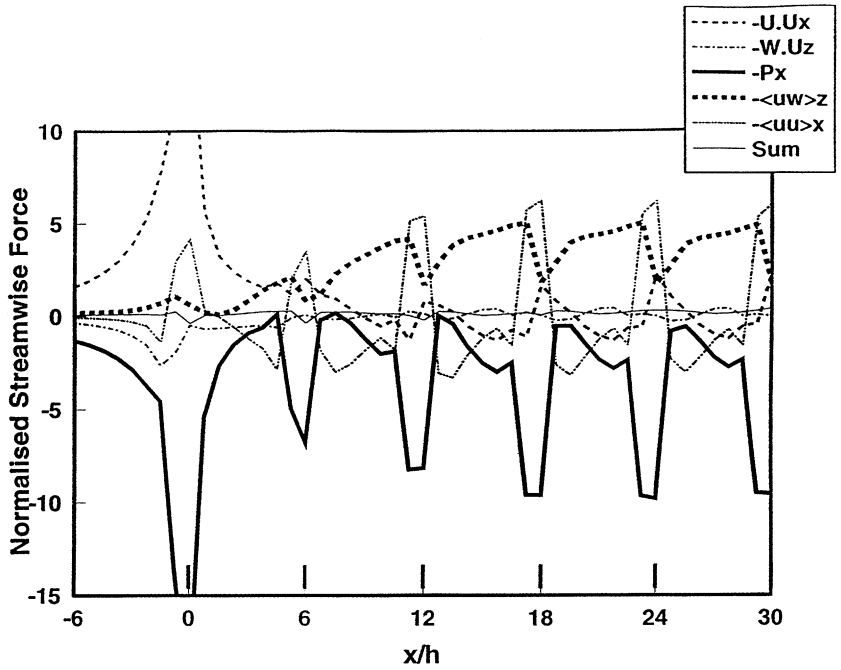

Fig. 5. Calculated horizontal profile at $z/h = 1/2$ of each term in the $\bar{u}$-momentum equation, normalized on u_{*0}^2/h. From the RWC closure corresponding to results shown in Figs. 2 and 3. The forces have been evaluated such that their sign indicates their contribution towards $\partial_t \bar{u}$; that is, negative terms exert a decelerating influence on the wind.

the calculated along-wind profiles of the individual terms in the $\bar{u}$-momentum budget, from the RWC closure. The fence drag term ($-k_r \bar{u}\sqrt{\bar{u}^2 + \bar{w}^2}$) has been lumped with the pressure gradient, and but for this, spikes of *positive* (favorable) pressure gradient would occur at (across) each barrier. The term in Fig. 5 labelled "Sum" is the residual imbalance, and it *should* vanish; it is non-zero only because the upwind finite difference here used to estimate the advection terms differs from SIMPLE's more refined scheme for fluxes across control volume faces.

It is evident from Fig. 5 that near the first windbreak, along-wind advection $\bar{u}\,\partial_x \bar{u}$ and pressure gradient $\partial_x \bar{p}$ are the dominant terms. The pressure gradient remains important close to downwind fences, but is largely annulled by almost a mirror-image pattern in the force $\partial_x \overline{u'^2}$, which results from the imposed TKE sink. Vertical advection is nowhere very important. Most significantly, the shear stress divergence $\partial_z \overline{u'w'}$ rises promptly downstream of the first windbreak to take the dominant place among these forces, except in the very near vicinity of each subsequent fence; everywhere it acts to re-accelerate the wind. Now whereas the pressure-gradient force is directly calculated by the numerical model (and seems to be in reasonable agreement with observations, Wilson, 1997), the shear stress is necessarily parameterized, this being the fundamental task of the 'turbulence closure' that is key to any RANS model. This is the reason for our hypothesis that the key problem with these poor simulations is the turbulence closure itself, rather than the treatment of momentum and TKE sinks.

6. Conclusion

The utility of micro- and agro-meteorology rests on knowledge of the wind. By some magic (often stemming largely from symmetry) the mess of detail that is turbulent flow must be squeezed into a manageably few robust relationships before a description of such interesting processes as, say, pollen transport,

can begin. When we address a process on a landscape that is not ideally flat and unobstructed (i.e. most of the real world) we may assume that wind models will be able to provide the needed spatial pattern of wind statistics, rather than an extensive (and expensive) program of measurements. But if we may hazard a generalization from the results given here, then it would be very unwise to place trust in present RANS wind models as a stand-alone alternative to measurements, in addressing processes in very disturbed micro-meteorological flows. Some meteorologists consider we need only await a fine-enough resolution in the mesoscale models, which is more or less the same as to say, enough computing power to push large eddy simulation (LES) towards other than the very limited flows presently within its grip. But the merit of such models for disturbed flows very much remains to be demonstrated, and there is a profound difficulty in how to parameterize the increasingly dominant subgrid turbulence, very near ground.

A reassessment of RANS wind models is timely because, particularly from the necessity to improve long term flux estimates from imperfect sites, micro-meteorologists increasingly are forced to accept that the idealization of horizontal uniformity is too obviously limiting—or wrong—to be ignored. And it is also important because technological society depends on models (particularly dispersion models, which usually ignore or näively parameterize flow disturbance) for the regulation of industry and the environment.

In this paper, we perhaps have bumped against a boundary, between the do-able and the not do-able, for RANS models in micro-meteorology.

Acknowledgements

This work was supported in part by the Natural Sciences and Engineering Research Council of Canada (NSERC). We thank Drs. Y. Zhuang and J. Argete, who performed the wind tunnel determination of the resistance coefficient of the McAneney–Judd windbreak cloth (and Dr. D.J. Wilson for use of the wind tunnel facility).

We hope this somewhat inconclusive paper is not amiss in a volume which honours George Thurtell, from the perspective that George's work has always been grounded in measurements, with a constant (and skeptical) attention to the limits of accuracy, of both measurements and modeling.

References

Ayotte, K.W., Finnigan, J.J., Raupach, M.R., 1998. A second-order closure for neutrally stratified vegetative canopy flows. Boundary Layer Meteorol. 90, 189–216.

Batchelor, G.K., 1953. The Theory of Homogeneous Turbulence. Cambridge University Press, Cambridge.

Bink, N.J., 1996. The structure of the atmospheric surface layer subject to local advection. Ph.D. thesis, Wageningen Agricultural University, 206 pp. (ISBN 90-5485-513-4).

Bradley, E.F., Mulhearn, P.J., 1983. Development of velocity and shear stress distributions in the wake of a porous shelter fence. J. Wind Eng. Ind. Aerodyn. 15, 145–156.

Brandle, J.R., Hintz, D.L., Sturrock, J.W., 1988. Windbreak technology. Agric. Ecosyst. Environ., vols. 22–23.

Cowan, I.R., Castro, I.P., Robins, A.G., 1997. Numerical considerations for simulations of flow and dispersion around buildings. J. Wind Eng. Ind. Aerodyn. 67–68, 535–545.

Craft, T.J., Launder, B.E., Suga, K., 1996. Development and application of a cubic eddy viscosity model of turbulence. Int. J. Heat Fluid Flow 17, 108–115.

Durst, F., Rasogi, A.K., 1980. Turbulent flows over two-dimensional fences. In: Turbulent Shear Flows, vol. 2 (Selected Papers from the Second International Symposium on Turbulent Shear Flows, London, 1979). Springer-Verlag, Berlin.

Hagen, L.J., Skidmore, E.L., Miller, P.L., Kipp, J.E., 1981. Simulation of effect of wind barriers on windflow. Trans. ASAE 24, 1002–1008.

Iqbal, M., Khatry, A.K., Seguin, B., 1977. A study of the roughness effects of multiple windbreaks. Boundary Layer Meteorol. 11, 187–203.

Judd, M.J., Raupach, M.R., Finnigan, J.J., 1996. A wind tunnel study of turbulent flow around a single and multiple windbreak. Part 1. Velocity fields. Boundary Layer Meteorol. 80, 127–165.

Kaiser, H., 1959. Die stromung an windshutzstreifen [The airflow through shelterbelts]. Berichte Deutscher Wetterdienstes.

Launder, B.E., Reece, G.J., Rodi, W., 1975. Progress in the development of a Reynolds stress turbulence closure. J. Fluid Mech. 68, 537–566.

Lee, S.-J., 2001. A numerical study on flow around a triangular prism located behind a porous fence. Fluid Dyn. Res. 28, 209–221.

McAneney, K.J., Judd, M.J., 1991. Multiple windbreaks: an aeolean ensemble. Boundary Layer Meteorol. 54, 129–146.

Packwood, A.R., 2000. Flow through porous fences in thick boundary layers: comparisons between laboratory and numerical experiments. J. Wind Eng. Ind. Aerodyn. 88, 75–90.

Patankar, S.V., 1980. Numerical Heat Transfer and Fluid Flow. Hemisphere, New York (ISBN 0-07-0487404).

Patton, E.G., Shaw, R.H., Judd, M.J., Raupach, M.R., 1998. Large eddy simulation of windbreak flow. Boundary Layer Meteorol. 87, 275–306.

Pinard, J.-P., Wilson, J.D., 2001. First- and second-order closure models for wind in a plant canopy. J. Appl. Meteorol. 40, 1762–1768.

Raine, J.K., Stevenson, D.C., 1977. Wind protection by model fences in a simulated atmospheric boundary layer. J. Ind. Aerodyn. 2, 159–180.

Rao, K.S., Wyngaard, J.C., Cote, O.R., 1974a. Local advection of momentum, heat, and moisture in micro-meteorology. Boundary Layer Meteorol. 7, 331–348.

Rao, K.S., Wyngaard, J.C., Cote, O.R., 1974b. The structure of the two-dimensional internal boundary layer over a sudden change of surface roughness. J. Atmos. Sci. 31, 738–746.

Rhie, C.M., Chow, W.L., 1983. A numerical study of the turbulent flow past an isolated airfoil with trailing edge separation. AIAA J. 21, 1525–1532.

Roache, P.J., 1997. Quantification of uncertainty in computational fluid dynamics. Ann. Rev. Fluid Mech. 29, 123–160.

Rubinstein, R., Barton, J.M., 1990. Non-linear Reynolds stress models and the renormalization group. Phys. Fluids A 2, 1472–1476.

Seginer, I., Mulhearn, P.J., Bradley, E.F., Finnigan, J.J., 1976. Turbulent flow in a model plant canopy. Boundary Layer Meteorol. 10, 423–453.

Seguin, B., Gignoux, N., 1974. Etude experimentale de l'influence d'un reseau de brise-vent sur le profl vertical de vitesse du vent [Experimental study of the effects of a network of windbreaks on the vertical profile of windspeed]. Agric. For. Meteorol. 13, 15–23.

Sini, J.-F., Anquetin, S., Mestayer, P.G., 1996. Pollutant dispersion and thermal effects in urban street canyons. Atmos. Environ. 30, 2659–2677.

Speziale, C.G., 1987. On non-linear k–l and k–ϵ models of turbulence. J. Fluid Mech. 178, 459–475.

Tani, N., 1958. On the wind tunnel test of the model shelter-hedge. Bull. Natl. Inst. Agric. Sci. Jpn. Ser. A 6, 75–80 (Summary in English).

Taylor, P.A., 1970. A model of airflow above changes in surface heat flux, temperature and roughness for neutral aud unstable conditions. Boundary Layer Meteorol. 1, 18–39.

van Eimern, J., Karschon, R., Razumova, L.A., Robertson, G.W., 1964. Windbeaks and shelterbelts. Technical Note, No. 59, World Meteorological Organization.

Wang, H., Takle, E.S., 1995. A numerical simulation of Boundary Layer flows near shelterbelts. Boundary Layer Meteorol. 75, 141–173.

Wilson, J.D., 1985. Numerical studies of flow through a windbreak. J. Wind Eng. Ind. Aerodyn. 21, 119–154.

Wilson, J.D., 1987. On the choice of a windbreak porosity profile. Boundary Layer Meteorol. 38, 37–49.

Wilson, J.D., 1988. A second-order closure model for flow through vegetation. Boundary Layer Meteorol. 42, 371–392.

Wilson, J.D., 1997. A field study of the mean pressure about a windbreak. Boundary Layer Meteorol. 85, 327–358.

Wilson, J.D., Flesch, T.K., 1999. Wind and tree sway in forest cutblocks. III. A windflow model to diagnose spatial variation. Agric. For. Meteorol. 93, 259–282.

Wilson, J.D., Mooney, C.J., 1997. Comments on 'A numerical simulation of boundary layer flows near shelterbelts' by H. Wang and E. Takle. Boundary Layer Meteorol. 85, 137–149.

Wilson, N.R., Shaw, R.H., 1977. A higher-order closure model for canopy flow. J. Appl. Meteorol. 16, 1197–1205.

Wilson, J.D., Swaters, G.E., Ustina, F., 1990. A perturbation analysis of turbulent flow through a porous barrier. Q. J. R. Meteorol. Soc. 116, 989–1004.

Wilson, J.D., Finnigan, J.J., Raupach, M.R., 1998. A first-order closure for disturbed plant canopy flows, and its application to windflow through a canopy on a ridge. Q. J. R. Meteorol. Soc. 124, 705–732.

Wilson, J.D., Flesch, T.K., Harper, L.A., 2001. Micro-meteorological methods for estimating surface exchange with a disturbed windflow. Agric. For. Meteorol. 107, 207–225.

Woodruff, N.P., Zingg, A.W., 1955. A comparative analysis of wind tunnel and atmospheric airflow patterns about single and successive barriers. Trans. Am. Geophys. Union 36, 203–208.

Wyngaard, J.C., 1981. Cup, propeller, vane, and sonic anemometers in turbulence research. Ann. Rev. Fluid Mech. 13, 399–423.

Yakhot, V., Orszag, S.A., Thangam, S., Gatski, T.B., Speziale, C.G., 1992. Development of turbulence models for shear flows by a double expansion technique. Phys. Fluids A 4, 1510–1520.

Yoshizawa, A., 1984. Statistical analysis of the deviation of the Reynolds stress from its eddy viscosity representation. Phys. Fluids 27, 1377–1387.